EXPERIMENTAL STUDY

Potential of healing a transected anterior cruciate ligament with genetically modified extracellular matrix bioscaffolds in a goat model

Matthew B. Fisher · Rui Liang · Ho-Joong Jung · Kwang E. Kim · Giovanni Zamarra · Alejandro J. Almarza · Patrick J. McMahon · Savio L-Y. Woo

Abstract

Purpose Biological augmentation to heal a torn anterior cruciate ligament (ACL) has gained significant interest. This study examined the potential advantages of using extracellular matrix (ECM) bioscaffolds from galactosyl-$\alpha(1,3)$galactose deficient pigs to heal the transected ACL.

Methods In 16 skeletally mature goats, the ACL in the right hindlimb was transected and repaired. In 9 of these animals, an ECM sheet was wrapped around the injury site and with an ECM hydrogel injected into the transected site. The remaining 7 animals were treated with suture repair only. The left hindlimb served as a sham-operated control.

Results After 12 weeks, the healing ACL in the ECM-treated group showed an abundance of continuous neo-tissue formation, while only limited tissue growth was found after suture repair only. The cross-sectional area of the ACL from the ECM-treated group was similar to sham-operated controls (n.s.) and was 4.5 times those of the suture repair group ($P < 0.05$). The stiffness of the femur-ACL-tibia complexes from the ECM-treated group was 2.4 times those of the suture repair group ($P < 0.05$). Furthermore, these values reached 48% of the sham-operated controls (53 ± 19 N/mm and 112 ± 21 N/mm, respectively, $P < 0.05$).

Conclusions The application of an ECM bioscaffold and hydrogel was found to accelerate the healing of a transected ACL following suture repair in the goat model with limited tissue hypertrophy and improvement in some of its biomechanical properties. Although more work is necessary to fully restore the function of the normal ACL, these early results offer a potential new approach to aid ACL healing.

M. B. Fisher · R. Liang · H.-J. Jung · K. E. Kim · G. Zamarra ·
A. J. Almarza · P. J. McMahon · S. L.-Y. Woo (✉)
Department of Bioengineering, Musculoskeletal Research
Center, Swanson School of Engineering,
University of Pittsburgh, 405 Center for Bioengineering,
300 Technology Drive, Pittsburgh, PA 15219, USA
e-mail: ddecenzo@pitt.edu

H.-J. Jung
Department of Orthopaedic Surgery, College of Medicine,
Chung-Ang University, Seoul, Korea

Introduction

Surgical reconstruction using soft-tissue autografts has been the standard of care for a torn anterior cruciate ligament (ACL). Although these autografts can restore initial knee stability, there are still a number of associated issues [34]. In fact, 20–25% of patients had less than satisfactory results in the long term, with clinical studies demonstrating premature osteoarthritic changes in the knee [3, 9, 16]. Thus, there is a persistent need to develop better treatment regimens for improved patient outcome.

With the advent of functional tissue engineering, there is a renewed hope to enhance healing and regeneration of the ACL by means of cells, growth factors, and scaffolds [2, 4, 39]. A successfully healed ACL would have many advantages over ACL reconstruction. Not only could the ligament's broad insertion sites and other complex anatomical features be preserved, but also issues related to donor site morbidity, the healing of the tendon graft in the bone tunnel, and tunnel placement could be eliminated.

Recently, surgeons have used blood derived from microfractures at the femoral insertion of the ACL to promote clotting and stimulate healing of an injured ACL [14, 35]. Encouraging results were obtained, and these authors attributed their success to hematoma formation and the recruitment of cells to the injury site. Using a similar strategy, a collagen-platelet composite (CPC) scaffold in combination with suture repair has also shown promise in animal studies [17].

An alternative to improve healing of ligaments and tendons is the use of extracellular matrix bioscaffolds (ECM) [19, 24, 44]. The porcine small intestinal submucosa (ECM–SIS), with its preferentially aligned type I collagen and bioactive agents (e.g. growth factors and chemoattractants) [5], has been shown to improve healing of a gap injury in the rabbit medial collateral ligament (MCL) with the tangent modulus and ultimate tensile strength of the MCL tissue closer to normal [24, 44]. Furthermore, when applied to a central third defect of the patellar tendon (PT) in the rabbit model, ECM–SIS could increase tissue formation and improve the stiffness and ultimate load of the bone-PT-bone complex [19]. More recently, the presence of TGF-β, bFGF, VEGF, PDGF, and IGF [23] was found in these ECMs, which can act as stimulators of cellular activity within ECM bioscaffolds and hydrogels. Additionally, others have shown that as ECM bioscaffolds degrade, its byproducts are able to stimulate cellular migration [31, 37].

In this study, the objective was to extend the application of an ECM–SIS bioscaffold to heal an injured ACL. The rationale was that an ECM sheet wrapped around the transected ACL would help tissue growth by isolating the healing tissue from the harsh synovial environment while limiting excessive tissue hypertrophy. The ECM was also prepared in a hydrogel form [12], so that it could be injected easily into the injury site to further accelerate healing through its chemoattractants [23, 31, 37]. When combined, it was hypothesized that the ECM hydrogel and ECM sheet can encourage rapid neo-tissue formation, while limiting its hypertrophy. Thus, healing of the ACL could take place such that its biomechanical properties as well as the joint function could be improved. To test this hypothesis, the ACL in the goat stifle joint was transected and treated with both an ECM bioscaffold and hydrogel. At 12 weeks, assessments included the joint stability [anterior-posterior tibial translation (A-PTT)] and in situ force of the healing ACL as well as the amount of neo-tissue formation, its morphology, and the biomechanical properties of the femur-ACL-tibia complexes (FATC) compared to those treated with suture repair alone.

Materials and methods

A total of 18 skeletally mature female Spanish breed goats with body mass of 42.6 $\pm$ 4.9 kg (mean $\pm$ SD) were used. The use of animals for this study was approved by the University of Pittsburgh's Institutional Animal Care and Use Committee. Early in the study, surgical error occurred in two animals, and they were excluded from further study. For the remaining sixteen goats, 9 were assigned to the ECM-treated group and 7 for the suture repair group. Two of the animals from each group were utilized for histological evaluation, while the rest were used for biomechanical evaluation.

This study employed ECM–SIS from genetically modified pigs in which the galactosyl-α(1,3)galactose (αGal) epitope is deficient, in order to reduce the potential for an acute immune response due to these porcine-derived scaffolds in patients [5, 8, 15, 27, 30]. To produce the ECM bioscaffolds, a small intestine from a knockout pig (Gal-Safe^{TM}, 13 mos., 180 kg.) was harvested immediately after euthanasia by Revivicor, Inc. and shipped overnight on dry ice. Once thawed, the ECM–SIS was separated from the small intestine, decellularized, lyophilized, and sterilized as previously described [13]. To make the ECM hydrogels, the processed ECM sheets were comminuted to a powder and enzymatically digested [12, 13]. The resultant pre-gel solution (10 mg/ml of ECM) was kept frozen at -20°C until needed.

All surgical procedures were performed using sterile techniques under general endotracheal anesthesia using isoflurane. The ACL in the right knee was transected throughout its entire cross-section and surgically repaired. No ACL tissue was removed. The contralateral leg served as a sham-operated control, in which the joint was opened, the ACL was visually observed (but not transected), and then, the wound was closed using sutures.

For the ECM-treated group, the ECM sheet was trimmed ($\sim$20 mm $\times$ $\sim$5 mm) and sutured to a similarly sized fibrin sponge (Surgifoam, Johnson and Johnson) via 4–0 non-absorbable sutures (Ethicon, Inc.) such that the luminal side of the ECM faced away from the fibrin sponge (Fig. 1b). The ECM hydrogel was formed by mixing 0.1 N NaOH, 10$\times$ PBS, 1$\times$ PBS, and the pre-gel solution at 4°C to reach an ECM concentration of 6 mg/ml and allowed to gel at 37°C [12].

Suture repair of the ACL was performed using a #1 Ethibond suture (Ethicon, Inc.). One suture was used for the proximal side, and one was used for the distal side. Each suture was passed through the tissue three times, such that two free ends were created to pass through the bone tunnels as shown in Fig. 1a. The first pass was made at least 5 mm from the injury site, and the passes were
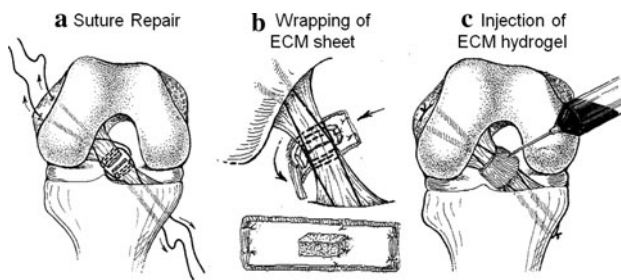
Fig. 1 Details on **a** surgical repair and application of **b** ECM bioscaffold and **c** ECM hydrogel

separated by approximately 2 mm along the length of the ligament. Next, two femoral tunnels were created by aiming a 1.5-mm guide wire at different angles immediately anterior to the insertion of the ACL. Two tibial tunnels were created using a 1.5-mm guide wire and a drill guide system placed immediately medial and lateral to the tibial insertion of the ACL. This technique allowed the bone tunnels to exit ~ 5 mm apart, creating a bone bridge. The sutures were passed through the bone tunnels and loosened. Next, the ACL was fully transected in its midsubstance between the repair sutures (Fig. 1a). In the ECM-treated group, the ECM sheet and fibrin sponge were placed posterior to the ACL stumps, with the fibrin sponge facing the injury site. For both the ECM-treated and suture repair groups, the repair sutures were tied over the bone bridges at 60° of joint flexion under manual tension. For the ECM-treated group, the ECM sheet and fibrin sponge were then wrapped around the ACL and sutured to enclose the injury site (Fig. 1b). After, the ECM hydrogel (2–3 ml) was injected into the injury site (Fig. 1c). Lastly, the wounds were closed using standard suture technique.

Postoperatively, all animals were allowed free cage activity, and the status of weight-bearing and general health of all goats was monitored. After 12 weeks, the goats were humanely euthanized. This time point was chosen in this study since it was long enough to enter the remodeling phase of healing and quantitatively assess the biomechanical properties of the healing tissue. For biomechanical testing, both hindlimbs were disarticulated at the hip joint, sealed in double plastic bags, and immediately stored at -20°C. Prior to testing, each stifle joint was thawed and prepared for biomechanical testing [1]. The specimens were kept moist with 0.9% saline throughout testing.

To examine the effects of ECM treatment on joint kinematics and in situ forces in the healing ACL, a robotic/universal force-moment sensor (UFS) testing system was used, as previously described [1, 25, 26, 29, 32, 40]. This testing system can accurately record the 6 degree of freedom (DOF) motion of the stifle joint using the robotic manipulator (Puma Model 762, Unimate, Inc.) as well as

apply and measure forces and moments to the stifle joint in 6-DOF via the UFS (Model 4015, JR3, Inc., Woodland, CA). To provide a reference position, a path of passive flexion–extension of the joint from full extension to 90° of joint flexion was first determined by minimizing all external forces and moments in the joint. After, an external 67-N anterior-posterior (A-P) tibial load was applied to the joint at 30°, 60°, and 90° of joint flexion, while the resulting 5 DOF joint kinematics (including A-P tibial translation) were measured [1, 40]. To determine the in situ force in the healing ACL, all other soft-tissue structures in and around the joint were dissected, leaving only the FATC. The articulating surfaces of the femoral condyles were also removed to eliminate bony contact. The previously recorded kinematics was repeated by the robotic manipulator while the UFS directly recorded the in situ force in the ACL [1, 40].

All FATCs used for the evaluation of joint function were further prepared for uniaxial tensile testing, as previously described [1]. First, the cross-sectional area of the healing and sham-operated ACLs was measured by means of a laser micrometer system [21, 41]. Subsequently, each specimen was mounted on a uniaxial tensile testing machine (model 4502; Instron, Canton, MA, USA) using customized clamps. Care was taken to ensure that each FATC specimen was positioned such that the anatomical orientation of the ACL was aligned along the axis of the applied tensile load [1, 42]. Each specimen was also aligned at ~ 70° of joint flexion. After a preload of 2 N was applied, the gauge length was reset to 0 mm. Each FATC underwent preconditioning by cyclically loading between 0 and 1 mm for 10 cycles. These parameters were chosen based on preliminary studies that showed about 1–1.5 mm of elongation was needed to reach the end of the toe region of the load-elongation curve. This level also allowed all tissues to reach a steady-state level of hysteresis without damaging the tissues. A second 2-N preload was applied, and the gauge length was reset. Then, the FATC was loaded until failure at 10 mm/min [43]. The failure of each specimen was visualized and recorded during the test and further reviewed on video images. From the load-elongation curve for each specimen, the ultimate load, i.e. maximum load, and ultimate elongation, i.e. the elongation corresponding to the ultimate load, were found. The stiffness was defined as the slope of the linear region of the load-elongation curve such that the $R^2 > 0.995$ when comparing the linear slope and the experimental data.

For histological examination ($n = 2$ per group), the ACLs were examined grossly, carefully removed at the insertion sites at the femur and tibia, embedded in O.C.T. compound, and frozen immediately in liquid nitrogen following euthanasia. Serial longitudinal and transverse cryosections of 8 μm thickness were cut through the

healing tissue. Slides were stained with hematoxylin and eosin and observed under a light microscope.

Statistical analysis

For statistical analyses, a Kolmogorov–Smirnov test was first done to ensure normality of the data on A-PTT, in situ force of the ACL, and cross-sectional area of the ACL as well as the stiffness, ultimate load, and ultimate elongation of the FATC. Then, a paired t test was performed to compare the experimental groups to their respective intact joint controls. For comparisons between experimental groups, data were normalized to the values for their sham-operated controls, followed by an unpaired t test. Significance was set overall at $P < 0.05$.

Results

All goats tolerated surgery well and could ambulate with a slight limp within a few hours following surgery. Daily inspection of the animals showed normal gait with full weight-bearing on all four limbs within the first 2 weeks.

The stifle joint function for the experimental and sham-operated control groups as measured by the robotic/UFS testing system is represented by the A-PTT plotted against the applied 67-N A-P tibial load at 30° of flexion (see Fig. 2a). All curves begin at the 67-N posterior tibial loads to provide a consistent reference position. Compared to the sham-operated group, the curves for the experimental groups were nonlinear and had higher values of A-PTT at each level of the applied anterior tibial load, with the most marked differences in the suture repair group. In terms of the total amount of A-PTT, both experimental groups had statistically higher values compared to those for the sham-operated controls at 30°, 60°, and 90° of flexion (Table 1, $P < 0.05$). Statistical significance between the ECM-treated and suture repair groups could not be determined at any of the flexion angles tested (n.s.).

In terms of the in situ force of the ACL, its anterior component under the 67-N anterior tibial load was plotted against the amount of A-PTT at 30° of flexion (see Fig. 2b). For consistency, the A-PTT for all groups was normalized to the respective sham-operated control group. The sham-operated ACLs carried the vast majority of the applied anterior tibial load. A similar response was found for the ECM-treated healing ACLs; however, the suture repaired ACLs carried less anterior force. Quantitatively, the values of the resultant in situ force of the healing ACL for both experimental groups were highest at 30° and 60° of flexion and were not statistically significant from their respective sham-operated controls (Table 2, n.s.). In fact, for the ECM-treated group, the in situ force in the healing
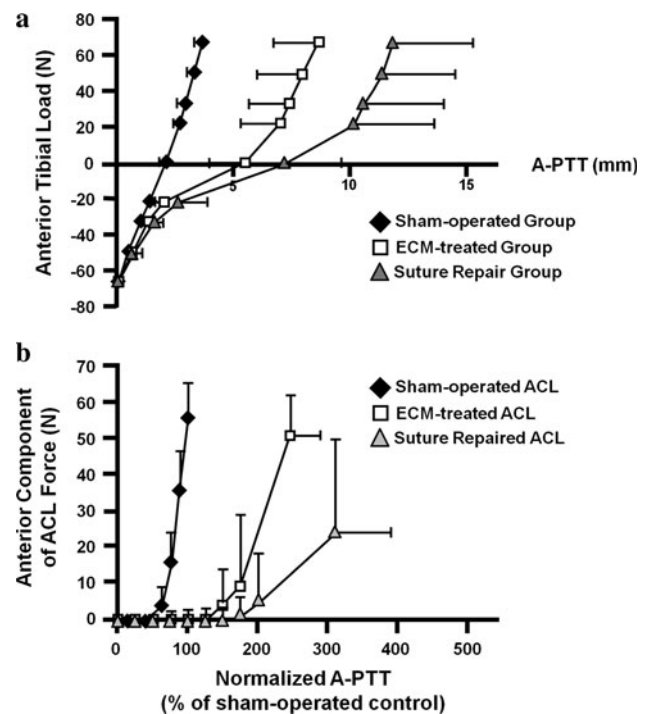

Fig. 2 a Average curves for the anterior-posterior tibial translation (A-PTT) in response to the 67-N A-P tibial load at 30° of flexion. Positive and negative force values indicate anterior and posterior tibial loads, respectively. **b** Anterior component of the in situ force of the ACL as a function of A-PTT at 30° of flexion. Values of A-PTT are normalized to those for the respective sham-operated control

Table 1 Anterior-posterior tibial translations (mm) of the goat stifle joints at 30°, 60°, and 90° of joint flexion under an 67-N anterior-posterior tibial load (mean ± SD)

	Joint flexion angle		
	30°	60°	90°
I. ECM-treated group			
Sham-operated control	3.4 ± 0.4	3.9 ± 0.5	3.0 ± 0.5
Experimental	8.6 ± 2.0*	11.3 ± 2.1*	10.2 ± 1.9*
II. Suture repair group			
Sham-operated control	3.8 ± 0.2	4.1 ± 0.3	2.8 ± 0.4
Experimental	11.8 ± 3.4*	14.4 ± 4.2*	10.8 ± 3.3*

* $P < 0.05$ compared to the respective sham-operated controls

ACL was found to be 84 and 96% of those for the sham-operated ACLs at 30° and 60°, respectively. At 90° of flexion, both experimental groups had significantly lower values compared to their respective sham-operated controls ($P < 0.05$). Like the joint kinematics, no statistically significant differences could be determined between experimental groups (n.s.).

After dissection, it was found that all ECM-treated ACLs healed with continuous neo-tissue formation and no noticeable concavities (Fig. 3b). The neo-tissues were

Table 2 Resultant in situ force of the ACL (N) at 30°, 60°, and 90° of joint flexion under a 67-N anterior tibial load (mean ± SD)

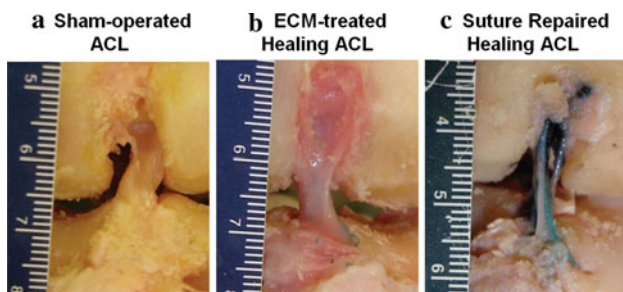|	Joint flexion angle		
	30°	60°	90°
I. ECM-treated group			
Sham-operated control	62 ± 5	54 ± 6	53 ± 5
Experimental	52 ± 11	52 ± 8	31 ± 12*
II. Suture repair group			
Sham-operated control	50 ± 12	51 ± 11	53 ± 7
Experimental	26 ± 24	29 ± 25	13 ± 15*

* $P < 0.05$ compared to the respective sham-operated controls

Fig. 3 Gross morphology of (**a**) sham-operated ACL, (**b**) ECM-treated healing ACL, and (**c**) suture repaired healing ACL at 12 weeks of healing

Fig. 4 The cross-sectional area of healing ACLs for the ECM-treated and suture repair groups at 12 weeks post-surgery normalized by the values for the respective sham-operated ACLs (*$P < 0.05$). Examples of the cross-sectional shape are also shown

Fig. 5 Histological appearance of (**a**) sham-operated ACL, (**b**) ECM-treated healing ACL, and (**c**) suture repaired healing ACL at 12 weeks of healing (×100 magnification, specimen identification numbers in *parentheses*). For the experimental groups, two specimens are shown to note the inter-specimen variability

slightly reddish in color and less opaque than the sham-operated control ACLs, which were white and consisted of distinct bundles with clearly observable collagen fiber orientation (Fig. 3a). Careful inspection revealed that the repair sutures were generally loose and elongated. There was no excessive hypertrophy of the ECM-treated ACLs, and the cross-sectional area was comparable to the sham-operated control group (29.0 ± 19.3 mm² vs. 23.0 ± 4.6 mm², respectively, n.s.). It should be noted that there was only a small amount of neo-tissue formation in the suture repair group (Fig. 3c). In fact, the average cross-sectional area of the healing ACLs in the suture repair group was only 34% of the average cross-sectional area for the sham-operated control group (6.5 ± 4.3 mm² vs. 21.6 ± 5.6 mm², respectively, $P < 0.05$). When the data were normalized by the respective sham-operated control of each animal [experimental/control (E/C)], the cross-sectional area values from the ECM-treated group were 4.5 times those of the suture repair group (127 ± 90% vs. 34 ± 25%, respectively, $P < 0.05$; see Fig. 4).

Histologically, the midsubstance of the ACL in the sham-operated group showed compact collagen fibers that were highly aligned with many regularly interspersed spindle-shaped cells (Fig. 5a). For the ECM-treated group, collagen fibers parallel to the longitudinal axis of the ligament were found wit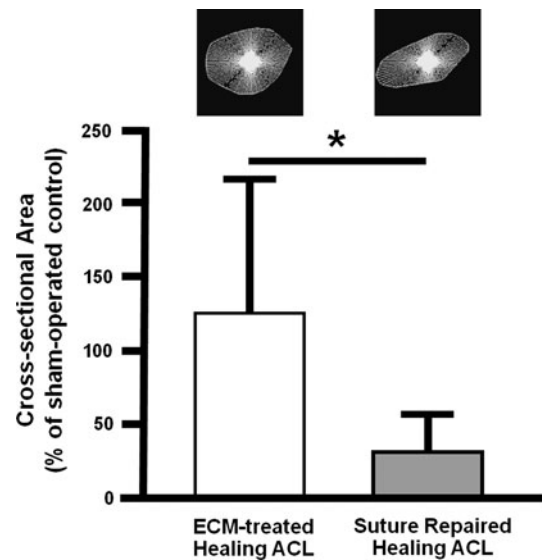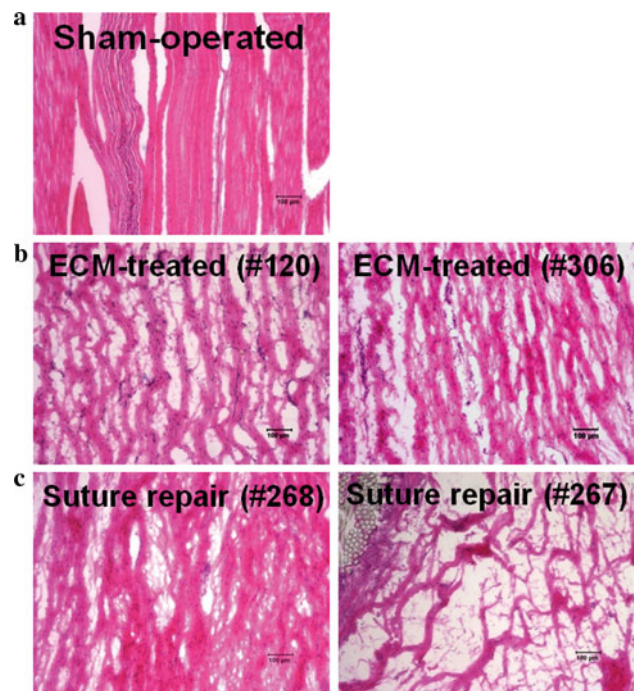h many spindle-shaped cells oriented along the collagen fibers (Fig. 5b). At this stage of healing, the matrix appeared as loose parallel strips of collagen fibers that were less dense with less relative alignment on a qualitative basis than that of the sham-operated group.

Moreover, transverse sections of the ECM-treated healing ACLs showed continuous tissue throughout its cross-section. For the suture repair group, large variability was observed with one specimen displaying a similar amount of matrix and fiber alignment as the ECM-treated group, while another specimen exhibiting very little healing with only sparse collagen fibers surrounding the repair sutures and less alignment than the ECM-treated group (Fig. 5c).

Tensile testing of the FATCs showed nonlinear load-elongation curves for the ECM-treated and suture repair groups (Fig. 6a). Typically, the toe region existed for up to 1–1.5 mm of elongation, followed by a linear region until failure. All healing specimens were found to fail in the tissue midsubstance of the healing ACL. The sutures

remained loose during tensile testing, and thus, the load-elongation curve was dominated by the healing tissue and not by the sutures. No clear separation at the insertion sites was observed. By 12 weeks, the structural properties of the FATCs as represented by the stiffness and ultimate load for both the ECM-treated and suture repair groups had not reached those of their respective sham-operated FATCs (Table 3, $P < 0.05$). For statistical comparisons between treatment groups, the normalized data (E/C) showed that the linear stiffness of the ECM-treated FATCs was 140% higher than that for the suture repair group ($48 \pm 19\%$ vs. $20 \pm 18\%$, respectively, $P < 0.05$; see Fig. 6b). No statistical significance could be determined between experimental groups in terms of ultimate load (n.s.).
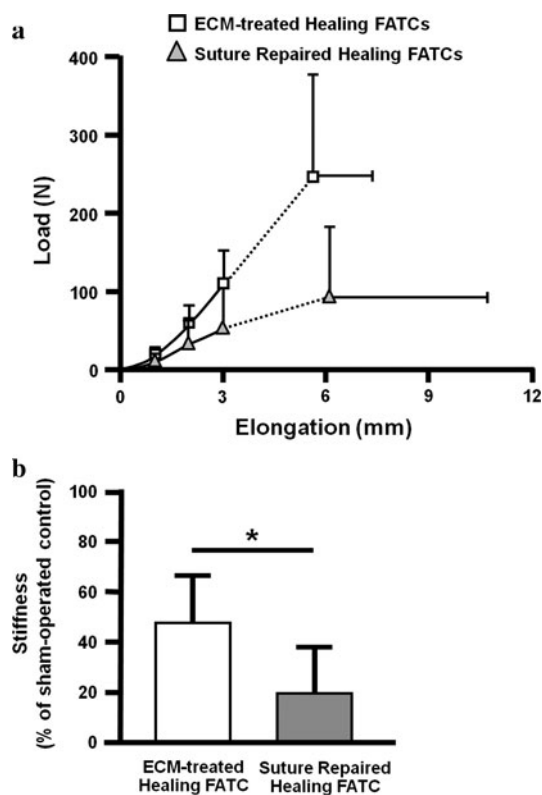

Fig. 6 a Average load-elongation curves of the ECM-treated and suture repair groups at 12 weeks post-surgery. **b** Stiffness of the healing FATC for the experimental groups as a percentage of the sham-operated controls at 12 weeks post-surgery (*$P < 0.05$)

Discussion

In this study, the potential of an ECM–SIS bioscaffold and its hydrogel to improve healing of a transected ACL following suture repair was demonstrated. The most important finding was that ECM treatment positively impacted the tensile properties of the healing FATC, as its stiffness was double that of the suture repair group. This is a direct result of the abundant neo-tissue formation and organized collagen fibers of the healing ACL following ECM treatment. The degradation byproducts of ECM–SIS, which have been shown to possess a number of bioactive agents such as growth factors and fibronectin, could have stimulated the cells to produce more de novo tissue [33]. Furthermore, ECM treatment did limit the healing ACL from hypertrophy as the cross-sectional area of the healing tissue was similar to the sham-operated ACL, which may have been due to the application of the ECM sheet wrapped around the injury site. This is a unique finding as other studies using biological augmentation could not limit excessive tissue hypertrophy [17]. Without excessive tissue growth, the quality of the healing tissue would improve during tissue remodeling in the long term [24, 44]. Collectively, these findings support the hypothesis. However, as no statistically significant differences could be found due to ECM treatment in terms of the ultimate load of the FATC as well as the A-PTT of the joint and in situ force of the

Table 3 Parameters representing the structural properties of the FATC at 12 weeks post-surgery (mean ± SD)

	ECM-treated group		Suture repair group	
	Sham-operated control	Experimental	Sham-operated control	Experimental
Stiffness (N/mm)	112 ± 21	$53 \pm 19^*$	125 ± 23	$24 \pm 21^*$
Ultimate load (N)	$1{,}624 \pm 235$	$249 \pm 129^*$	$1{,}385 \pm 360$	$95 \pm 90^*$
Ultimate elongation (mm)	15.3 ± 2.9	$5.6 \pm 1.7^*$	19.0 ± 6.3	$6.1 \pm 4.6^*$

* $P < 0.05$ compared to the respective sham-operated controls

healing ACL, the hypothesis was only partially confirmed. The A-PTT of the joint was reduced to some extent, although not restored, by the ECM treatment. With further improvements in design, it may be speculated this bioscaffold augmentation will at least positively contribute to the better joint stability. Further, it is important to note that even with ECM treatment, the biomechanical properties of the healing ACL at 12 weeks were still well below those of the normal FATC.

The values for A-PTT for the stifle joint with ECM treatment at 12 weeks postoperatively in the goat model were consistent with the literature using animal models even though they were 2–3 times greater than those of the intact joint [1, 7, 28]. The issue of increased joint instability following surgical treatment of an ACL injury is a common observation in most animal studies. For example, following ACL reconstruction and other tissue engineering approaches to heal a transected ACL, the A-PTT could range from 2 to 6 times those of the intact joint [1, 7, 17, 28]. The literature has attributed this increase to the lack of appropriate postoperative rehabilitation. Nevertheless, the increased joint instability remains an issue in this animal study, and much improvement in the properties of the healing ACL along with restoring joint stability is needed before clinical translation may be considered.

The biomechanical data for the healing FATC in the ECM-treated group compared favorably to those for other functional tissue engineering techniques as well as ACL reconstruction in animal models [1, 7, 17, 28]. The stiffness was similar to those treated with the CPC scaffold following suture repair in a porcine model at 3 months (53 ± 19 N/mm vs. 40.2 ± 21.8 N/mm, respectively) [17]. Moreover, the structural properties of FATC also compared favorably to those following ACL reconstruction in terms of both stiffness (53 ± 19 N/mm vs. 37.2 ± 22.0 N/mm, respectively) and ultimate load (249 ± 129 N vs. 268.8 ± 175.8 N, respectively) [28].

Another contribution of this study was the use of genetically modified ECM, which could help to address the clinical concerns of chronic inflammation found in some patients following implantation of the porcine xenografts [15, 27]. A significant part of the inflammatory response has been attributed to the existence of the αGal epitope found in the porcine ECM [5, 8, 30], and αGal-deficient tissues from this genetically modified porcine model have been shown to limit the immune rejection response [6, 20, 45]. As such, the use of ECM from these αGal(−) pigs would greatly eliminate the immunogenicity in humans, making the porcine ECM a unique source for clinical applications.

The suture repair procedure chosen for this study was based on those utilized in the clinical literature [10, 18, 38]. It is important to note that the healing response following suture repair alone was highly variable, with 3 out of 7 animals having little or no tissue formation, which was in contrast to the ECM-treated group. This can be easily seen when comparing histological sections between two different animals (Fig. 5c) as well the biomechanical data, which precluded the ability to determine statistical significance in some cases. In the original study design, 7 goats were allocated for biomechanical evaluation following suture repair alone. Following testing of 5 of these animals, the large variability in the suture repair group was noted. A post hoc power analysis revealed that up to 15 goats per group would be needed to detect statistical differences in the A-PTT, in situ force of the ACL, and ultimate load of the FATC, which was unfeasible. As such, it was decided to better utilize the remaining animals in a separate study. Nevertheless, the small sample size in the suture repair group is a limitation of this study. However, with the current sample size, statistically significant differences in the cross-sectional area of the healing tissue as well as the stiffness of the healing FATC following ECM treatment were achieved.

There are other limitations to the current study. First, the amount and type of growth factors and chemoattractants released from the ECM, their release profiles, and the inter-specimen variability in their release are unknown for the current application. In the future, these mechanisms will be explored within the intra-articular environment during ACL healing as well as results at longer-term time points in more detail to more fully characterize the healing response. Second, the stresses and strains of the healing tissue, and thus its mechanical properties, were not measured, due to the presence of the sutures. Future studies will need to accurately obtain these data to assess the quality of the healing tissue in terms of its mechanical properties. Third, the potential for injury to the insertion sites and the proprioceptive nerve endings in the injured ACL following suture repair was not investigated, but must be considered in the future. Fourth, the externally applied loads used in the current study are similar to those used in clinical examination to evaluate ACL function and thus could not mimic those during in vivo activities. As a result, the data obtained do not provide a view of the function of the ACL during in vivo motion and must be treated with caution. Recently, several groups have developed highly accurate biplanar fluoroscopy to record in vivo joint kinematics [22, 36]. In the future, such kinematics data could be repeated using a robotic/UFS testing system such that the in situ forces in the healing ACL during activities of daily living could be determined [40].

Nevertheless, the current study has demonstrated the potential of αGal(−) ECM bioscaffolds and hydrogels in combination with suture repair to help with ACL healing. The considerable neo-tissue formation without hypertrophy

and substantial biomechanical function of the healing ACL are indeed exciting. This novel approach can serve as a basis for future work such as ECM treatment in combination with suture augmentation techniques to better restore and maintain initial joint stability for ACL healing [11]. Additional studies will also examine the contribution of other tissues in and around the joint to A-P joint stability and assess how they are affected following ACL injury and healing [26, 29, 32]. Finally, the reduced immune rejection potential of the genetically engineered ECM bioscaffolds from the porcine could not be tested in the current animal model but should offer an exciting avenue for further study in primate models with the distinct possibility for translation into clinical use. Although much work remains, this study supports the increasingly widespread concept among clinicians that biological augmentation, in this case the use of ECM bioscaffolds, could be utilized to stimulate healing of the ACL.

Conclusion

The application of an ECM bioscaffold and hydrogel was found to accelerate the healing of a transected ACL following suture repair in the goat model with limited tissue hypertrophy and improvement in some of its biomechanical properties. Although more work is necessary to fully restore the function of the normal ACL, these early results offer a potential new approach to aid ACL healing with the distinct possibility for clinical translation.

References

1. Abramowitch SD, Papageorgiou CD, Withrow JD, Gilbert TW, Woo SL-Y (2003) The effect of initial graft tension on the biomechanical properties of a healing ACL replacement graft: a study in goats. J Orthop Res 21(4):708–715
2. Agung M, Ochi M, Yanada S et al (2006) Mobilization of bone marrow-derived mesenchymal stem cells into the injured tissues after intraarticular injection and their contribution to tissue regeneration. Knee Surg Sports Traumatol Arthrosc 14(12):1307–1314
3. Anderson AF, Snyder RB, Lipscomb AB Jr (2001) Anterior cruciate ligament reconstruction. A prospective randomized study of three surgical methods. Am J Sports Med 29(3):272–279
4. Anitua E, Sanchez M, Orive G, Andia I (2007) The potential impact of the preparation rich in growth factors (PRGF) in different medical fields. Biomaterials 28(31):4551–4560
5. Badylak SF (2007) The extracellular matrix as a biologic scaffold material. Biomaterials 28(25):3587–3593
6. Chen G, Qian H, Starzl T et al (2005) Acute rejection is associated with antibodies to non-Gal antigens in baboons using Gal-knockout pig kidneys. Nat Med 11(12):1295–1298
7. Cummings JF, Grood ES (2002) The progression of anterior translation after anterior cruciate ligament reconstruction in a caprine model. J Orthop Res 20(5):1003–1008
8. Dai Y, Vaught TD, Boone J et al (2002) Targeted disruption of the alpha1,3-galactosyltransferase gene in cloned pigs. Nat Biotechnol 20(3):251–255
9. Drogset JO, Grontvedt T, Robak OR et al (2006) A 16-year follow-up of three operative techniques for the treatment of acute ruptures of the anterior cruciate ligament. J Bone Jt Surg Am 88(5):944–952
10. Feagin JA Jr, Curl WW (1976) Isolated tear of the anterior cruciate ligament: 5-year follow-up study. Am J Sports Med 4(3):95–100
11. Fisher MB, Jung HJ, McMahon PJ, Woo SL-Y (2010) Evaluation of bone tunnel placement for suture augmentation of an injured anterior cruciate ligament: effects on joint stability in a goat model. J Orthop Res 28(10):1373–1379
12. Freytes DO, Martin J, Velankar SS, Lee AS, Badylak SF (2008) Preparation and rheological characterization of a gel form of the porcine urinary bladder matrix. Biomaterials 29(11):1630–1637
13. Gilbert TW, Stolz DB, Biancaniello F, Simmons-Byrd A, Badylak SF (2005) Production and characterization of ECM powder: implications for tissue engineering applications. Biomaterials 26(12):1431–1435
14. Gobbi A, Bathan L, Boldrini L (2009) Primary repair combined with bone marrow stimulation in acute anterior cruciate ligament lesions: results in a group of athletes. Am J Sports Med 37(3):571–578
15. Iannotti JP, Codsi MJ, Kwon YW et al (2006) Porcine small intestine submucosa augmentation of surgical repair of chronic two-tendon rotator cuff tears. A randomized, controlled trial. J Bone Jt Surg Am 88(6):1238–1244
16. Jomha NM, Borton DC, Clingeleffer AJ, Pinczewski LA (1999) Long-term osteoarthritic changes in anterior cruciate ligament reconstructed knees. Clin Orthop Relat Res 358:188–193
17. Joshi SM, Mastrangelo AN, Magarian EM, Fleming BC, Murray MM (2009) Collagen-platelet composite enhances biomechanical and histologic healing of the porcine anterior cruciate ligament. Am J Sports Med 37(12):2401–2410
18. Kaplan N, Wickiewicz TL, Warren RF (1990) Primary surgical treatment of anterior cruciate ligament ruptures. A long-term follow-up study. Am J Sports Med 18(4):354–358
19. Karaoglu S, Fisher MB, Woo SL-Y et al (2008) Use of a bioscaffold to improve healing of a patellar tendon defect after graft harvest for ACL reconstruction: a study in rabbits. J Orthop Res 26(2):255–263
20. Kuwaki K, Tseng YL, Dor FJ et al (2005) Heart transplantation in baboons using alpha1,3-galactosyltransferase gene-knockout pigs as donors: initial experience. Nat Med 11(1):29–31
21. Lee TQ, Woo SL-Y (1988) A new method for determining cross-sectional shape and area of soft tissues. J Biomech Eng 110(2):110–114
22. Li G, Van de Velde SK, Bingham JT (2008) Validation of a non-invasive fluoroscopic imaging technique for the measurement of dynamic knee joint motion. J Biomech 41(7):1616–1622
23. Liang R, Fisher M, Yang G, Hall C, Woo SL-Y (2011) Alpha1,3-galactosyltransferase knockout does not alter the properties of porcine extracellular matrix bioscaffolds. Acta Biomater 7(4):1719–1727
24. Liang R, Woo SL-Y, Takakura Y et al (2006) Long-term effects of porcine small intestine submucosa on the healing of medial collateral ligament: a functional tissue engineering study. J Orthop Res 24(4):811–819

25. Livesay GA, Fujie H, Kashiwaguchi S et al (1995) Determination of the in situ forces and force distribution within the human anterior cruciate ligament. Ann Biomed Eng 23(4):467–474

26. Ma CB, Papageogiou CD, Debski RE, Woo SL-Y (2000) Inter-action between the ACL graft and MCL in a combined ACL + MCL knee injury using a goat model. Acta Orthop Scand 71(4):387–393

27. Malcarney HL, Bonar F, Murrell GA (2005) Early inflammatory reaction after rotator cuff repair with a porcine small intestine submucosal implant: a report of 4 cases. Am J Sports Med 33(6):907–911

28. Ng GY, Oakes BW, Deacon OW, McLean ID, Lampard D (1995) Biomechanics of patellar tendon autograft for reconstruction of the anterior cruciate ligament in the goat: 3-year study. J Orthop Res 13(4):602–608

29. Papageorgiou CD, Gil JE, Kanamori A et al (2001) The biome-chanical interdependence between the anterior cruciate ligament replacement graft and the medial meniscus. Am J Sports Med 29(2):226–231

30. Phelps CJ, Koike C, Vaught TD et al (2003) Production of alpha 1,3-galactosyltransferase-deficient pigs. Science 299(5605): 411–414

31. Reing JE, Zhang L, Myers-Irvin J et al (2009) Degradation products of extracellular matrix affect cell migration and prolif-eration. Tiss Eng Part A 15(3):605–614. doi:10.1089/ten.tea. 2007.0425

32. Sakane M, Livesay GA, Fox RJ et al (1999) Relative contribution of the ACL, MCL, and bony contact to the anterior stability of the knee. Knee Surg Sports Traumatol Arthrosc 7(2):93–97

33. Scherping SC Jr, Schmidt CC, Georgescu HI et al (1997) Effect of growth factors on the proliferation of ligament fibroblasts from skeletally mature rabbits. Connect Tiss Res 36(1):1–8

34. Spindler KP, Kuhn JE, Freedman KB et al (2004) Anterior cru-ciate ligament reconstruction autograft choice: bone-tendon-bone versus hamstring: does it really matter? A systematic review. Am J Sports Med 32(8):1986–1995

35. Steadman JR, Cameron-Donaldson ML, Briggs KK, Rodkey WG (2006) A minimally invasive technique ("healing response") to treat proximal ACL injuries in skeletally immature athletes. J Knee Surg 19(1):8–13

36. Torry MR, Shelburne KB, Peterson DS et al (2011) Knee kine-matic profiles during drop landings: a biplane fluoroscopy study. Med Sci Sports Exerc 43(3):533–541

37. Vorotnikova E, McIntosh D, Dewilde A et al (2010) Extracellular matrix-derived products modulate endothelial and progenitor cell migration and proliferation in vitro and stimulate regenerative healing in vivo. Matrix Biol 29(8):690–700

38. Warren RF (1983) Primary repair of the anterior cruciate liga-ment. Clin Orthop Relat Res 172:65–70

39. Wiig ME, Amiel D, VandeBerg J et al (1990) The early effect of high molecular weight hyaluronan (hyaluronic acid) on anterior cruciate ligament healing: an experimental study in rabbits. J Orthop Res 8(3):425–434

40. Woo SL-Y, Abramowitch SD, Kilger R, Liang R (2006) Bio-mechanics of knee ligaments: injury, healing, and repair. J Bio-mech 39(1):1–20

41. Woo SL-Y, Danto MI, Ohland KJ, Lee TQ, Newton PO (1990) The use of a laser micrometer system to determine the cross-sectional shape and area of ligaments: a comparative study with two existing methods. J Biomech Eng 112(4):426–431

42. Woo SL-Y, Hollis JM, Adams DJ, Lyon RM, Takai S (1991) Tensile properties of the human femur-anterior cruciate ligament-tibia complex: the effects of specimen age and orientation. Am J Sports Med 19(3):217–225

43. Woo SL-Y, Peterson RH, Ohland KJ, Sites TJ, Danto MI (1990) The effects of strain rate on the properties of the medial collateral ligament in skeletally immature and mature rabbits: a biome-chanical and histological study. J Orthop Res 8(5):712–721

44. Woo SL-Y, Takakura Y, Liang R, Jia F, Moon DK (2006) Treatment with bioscaffold enhances the fibril morphology and the collagen composition of healing medial collateral ligament in rabbits. Tiss Eng 12(1):159–166

45. Yamada K, Yazawa K, Shimizu A et al (2005) Marked prolon-gation of porcine renal xenograft survival in baboons through the use of alpha1,3-galactosyltransferase gene-knockout donors and the cotransplantation of vascularized thymic tissue. Nat Med 11(1):32–34